HHS Public Access

Author manuscript

Pharm Res. Author manuscript; available in PMC 2025 January 31.

Published in final edited form as:

Pharm Res. 2023 November ; 40(11): 2667–2675. doi:10.1007/s11095-023-03598-7.

Functional Evaluation of P-gp and Bcrp at the Murine Blood-Cerebrospinal Fluid Barrier

Austin Sun[a], **Joanne Wang**[a,*]

[a]Department of Pharmaceutics, University of Washington, Seattle, Washington 98195

Abstract

Purpose—The brain is protected from circulating metabolites and xenobiotics by the blood-brain barrier (BBB) and the blood-cerebrospinal fluid (CSF) barrier. Previous studies report that P-glycoprotein (P-gp) and breast cancer resistance protein (Bcrp) are expressed apically or subapically at the blood-CSF barrier (BCSFB), implying a paradoxical function to mediate blood-to-CSF transport of xenobiotics. As evidence of P-gp and Bcrp activity at the BCSFB is limited, the goal of this study is to investigate functional activity of P-gp and Bcrp at the murine BCSFB using a live tissue imaging approach.

Methods—The choroid plexuses (CP) forming the BCSFB were freshly isolated from mouse brain ventricles and incubated with fluorescent probes calcein-AM and BODIPY FL-Prazosin. Using quantitative fluorescence microscopy, the functional contributions of Bcrp and P-gp were examined using inhibitors and mice with targeted deletion of the *Abcb1a/b* or *Abcg2* gene.

Results—Apical transport of calcein-AM in choroid plexus epithelial (CPE) cells is sensitive to inhibition by elacridar and Ko143 but is unaffected by P-gp deletion. In wild-type mice, elacridar increased CPE accumulation of BODIPY FL-Prazosin by 220% whereas deletion of Bcrp increased BODIPY FL-Prazosin accumulation by 43%. There was no change in Mdr1a/1b mRNA expression in CP tissues from the $Bcrp^{-/-}$ mice.

Conclusions—This study demonstrated functional activity of Bcrp at the BCSFB apical membrane and provided evidence supporting an additional contribution by P-gp. These findings contribute to the understanding of transport mechanisms that regulate CSF drug concentrations, which may benefit future predictions of CNS drug disposition, efficacy, and toxicity.

Keywords

P-glycoprotein; Breast cancer resistance protein; Blood-CSF barrier; CNS pharmacokinetics; drug transport

[*]**Corresponding author**: Joanne Wang, Ph.D., University of Washington, Department of Pharmaceutics, H272 Health Sciences Building, Seattle, WA 98195-7610, Fax: (206) 543-3204, jowang@uw.edu.

AUTHOR CONTRIBUTIONS

Original study conception and design was completed by Joanne Wang and Austin Sun. Experiments were performed by Austin Sun, and data analysis was performed by Austin Sun and Joanne Wang. The initial draft of the manuscript was written by Austin Sun and critically revised by Joanne Wang.

CONFLICT OF INTEREST STATEMENT

The authors declare no competing financial interest.

INTRODUCTION

There is a high, unmet need for future treatments of neurological disorders, which are the primary cause of disability and the second leading cause of death worldwide (1). The brain is the most physiologically complex organ in the human body, which can lead to many obstacles during central nervous system (CNS) drug development. Diseases of the brain and greater CNS, such as Alzheimer's disease, may have complex pathologies and several potential pharmacological targets. CNS pharmacokinetics are also complex and poorly understood, which in part contributes to the high attrition rate during the development of CNS drugs (2).

Drug transporters play an important role in mediating drug-drug interactions, drug disposition, and toxicity (3). At the blood-brain barrier (BBB), efflux transporters such as P-glycoprotein (P-gp) and breast cancer resistance protein (BCRP) are expressed on the luminal membrane, where they limit the entry of their substrates into the brain (4,5). The importance of P-gp and BCRP in restricting drug brain penetration has been well documented (4). The two transporters have an overlapping substrate pool, thus P-gp and BCRP can synergistically limit the CNS penetration of shared substrates (4). P-gp and BCRP are also reportedly expressed in other blood-CNS barrier sites such as the blood-cerebrospinal fluid (CSF) barrier (5–7), implying a functional role beyond the BBB.

The blood-CSF barrier (BCSFB) is formed by the choroid plexuses (CP), which are comprised of a layer of polarized, tight junction-linked choroid plexus epithelial (CPE) cells that surround a core of fenestrated blood capillaries (8,9). The CPE cells express transporters and enzymes that contribute to xenobiotic and endobiotic clearance from the CSF (9). Several solute carrier transporters, including the peptide transporter 2 (PEPT2), organic anion transporter 3 (OAT3), and plasma membrane monoamine transporter (PMAT), are expressed at the apical (CSF-facing) membrane of the CPE cells and mediate drug uptake from the CSF into CPE cells (10–14). By influencing drug concentrations in the CSF, transporters at the BCSFB may also play a role in regulating the effective drug concentrations in the CNS.

Interestingly, previous studies have suggested that P-gp and BCRP are expressed apically (CSF-facing) or subapically at the BCSFB. Using immunohistochemistry and immunofluorescence approaches, BCRP has been localized apically in mouse CP (7,15), while P-gp has been localized apically or subapically in CP of rats and pigs (6,16). Since P-gp and BCRP are efflux transporters, their location at the apical membrane of CPE cells would imply a paradoxical role of mediating blood-to-brain transport of substrates, which is opposite to their functions at the BBB. Limited functional studies have been conducted using *in vitro* systems. Transport of calcein-AM, a P-gp probe, was sensitive to the P-gp inhibitor valspodar in cell lines of rat or human CP origin (17,18). Apical-to-basolateral transport of the P-gp substrate ^{99m}Tc-sestamibi increased with elacridar, a dual inhibitor for P-gp and Bcrp, in rat CPE primary cells cultured in a transwell system, suggesting P-gp activity at the apical CSF-facing membrane (6). However, two other P-gp substrates, rhodamine123 and verapamil, were not actively transported in porcine primary CPE cell culture (16). Evidence of BCRP function at the BCSFB is even more limited; a single study demonstrated that

transport of the BCRP substrate BODIPY FL-Prazosin was sensitive to the BCRP inhibitor Ko143 in cultured human choroid plexus papilloma cells (18). However, no directional difference in transport was observed when the cells were grown in a transwell system (18). Broadly, CPE cell cultures or immortalized CP cell lines have been shown to have altered transporter expression and reduced tight junction formation as compared to native CP tissue (17). Thus, there is an impetus to study P-gp and BCRP transport function at the BCSFB in a more physiologically relevant system.

Our laboratory recently developed and validated a quantitative fluorescence microscopy approach to study transcellular transport mechanisms of organic cations and organic anions at the murine BCSFB (19). This approach enables the study of real-time transport processes in freshly isolated intact CP tissues and can distinguish between transport processes at the apical and basolateral membranes (20). In this study, we first determined the relative mRNA expression of *Abcb1a/b* (P-gp or Mdr1a/1b) and *Abcg2* (Bcrp) in murine lateral ventricle CP tissues. Using quantitative fluorescence microscopy, we investigated the functional role of P-gp and Bcrp at the BCSFB using fluorescent probes in freshly isolated murine CP tissues. The contribution of P-gp and Bcrp were evaluated using established inhibitors and mouse models with targeted deletion of the *Abcb1a/b* or *Abcg2* gene.

MATERIALS AND METHODS

Chemicals and Materials

All chemicals purchased and used were of 95% or greater purity. Calcein-AM was purchased from Enzo Life Sciences (ENZ-52002, Farmingdale, NY). BODIPY FL-Prazosin was purchased from ThermoFisher Scientific (B7433, Waltham, MA). Ko143 was purchased from Medchemexpress (HY-10010, Monmouth Junction, NJ). Unless otherwise specified, all other chemicals were purchased from Sigma-Aldrich (St. Louis, MO). Animal handling supplies, PCR plates, confocal dishes, and other plastic wares were purchased from VWR (Radnor, PA).

Animals and Choroid Plexus Tissue Collection

Animal experiments were carried out in accordance with the Guide for the Care and Use of Laboratory Animals as adopted and promulgated by the U.S. National Institutes of Health and in accordance with animal protocols approved by the Institutional Animal Care and Use Committee at the University of Washington. Animals were housed in the specific pathogen free facility at the University of Washington and maintained under standard conditions, with food and water available ad libitum. FVB wild-type (FVB-M), FVB Bcrp$^{-/-}$ (2767-M), and Mdr1a/1b$^{-/-}$ (1487-M) mice were obtained from Taconic Biosciences (Germantown, NY). Generation and physiological characteristics of the transgenic strains have been described previously (21,22).

Adult (8-13 week old) male FVB wild-type and transgenic mice were euthanized by CO_2 inhalation, followed by decapitation. Mouse brain was isolated and maintained in ice cold artificial CSF (aCSF: 119 mM NaCl, 26.2 mM $NaHCO_3$, 2.5 mM KCl, 1 mM NaH_2PO_4, 1.3 mM $MgCl_2$, 2.5 mM $CaCl_2$, 10 mM glucose), previously gassed with 95% O_2/5% CO_2 for

tissue isolation. Lateral ventricle CP and 4th ventricle CP were isolated from mouse brain under a dissecting microscope using an approach previously described (20). CP tissue used for uptake experiments were then transferred into pre-gassed, ice-cold aCSF immediately after removal, while tissues used for real-time PCR were immediately flash frozen in liquid nitrogen and stored in a −80°C freezer until further processing.

Quantification of Transporter mRNA Expression by Real-time PCR

Frozen CP tissue was homogenized by a bead disruptor, and total RNA was extracted by RNeasy Mini Kit (Qiagen, Germantown, NY). Total RNA was then converted to cDNA by reverse transcription using the High-Capacity cDNA Reverse Transcription Kit (Applied Biosystems, Waltham, MA). Expression at the mRNA level of transporters at the CP was quantified using TaqMan Real-Time PCR Master Mix (Applied Biosystems, Waltham, MA) as described previously (14,19). The relative mRNA levels of these transporters in CP were normalized to glyceraldehyde-3-phosphate dehydrogenase (*Gapdh*).

Transport Imaging Studies in Choroid Plexus of Wild-type and Knockout Mice

Transport imaging studies using freshly isolated mouse lateral ventricle CP were performed using an approach previously described (19,20). Isolated CP tissues maintain vitality and transport activity for up to 2-3 hours after isolation (20), and all transport studies were performed within 2 hours after tissue isolation. Single time-point transport studies were initiated by adding the fluorescent compound in the presence or absence of an inhibitor into the aCSF. Incubations were carried out for 20 min in sealed Ziploc bags containing 95% O_2/5% CO_2. One to three undamaged observation areas containing both CPE cells and adjacent subepithelial region were selected, and the fluorescent signals were recorded. To record real-time transport of the fluorescent substrate, a specific observation area containing intact CPE cells and adjacent subepithelial region was selected and immobilized in pregassed aCSF. The experiment was initiated by adding a specified concentration of the fluorescent compound, and the fluorescent signals were recorded every minute for 20 minutes. Experiments were performed in individual CP tissues and repeated independently in CP tissues harvested from 3 or more animals.

Confocal Image Acquisition and Analysis

Image acquisition and analysis were performed using procedures as previously described (20). Briefly, imaging was performed using a Zeiss LSM 710 confocal microscope fitted with a Zeiss 40x, NA 1.3 oil immersion objective (total magnification: 400x). Brightfield imaging was used to identify observation areas containing CPE cells with adjacent blood capillaries. Samples containing BODIPY FL-Prazosin or calcein-AM were illuminated using a 488 nm fixed wavelength argon laser, with appropriate corresponding dichroic and emission filters to detect the emission of the fluorescent probes. Low laser intensity (5% of maximum) was used to minimize sample photobleaching. Laser gain and offset was set such that autofluorescence of tissue was minimally detectable. Confocal images were captured as 15 sec scans at 1024 × 1024 resolution, 16 frames line-averaged, with a pixel dwell of 0.79 μsec. Replicate studies were performed using the same objective lens, identical laser power, and identical detector settings.

Digital image analysis was performed using Fiji ImageJ (1.53t) (23) and performed as described previously (20).

Choroid plexus efflux index (CPEI) at 20 minutes ($CPEI_{20min}$) was calculated according to the following formula (20):

$$CPEI_{20min}(\%) = \frac{\sum pixel\ \ intensity_{se}}{\sum pixel\ \ intensity_{cells+se}}$$

$CPEI_{20min}$ is expressed as a percentage, where Σpixel $intensity_{se}$ is the sum average pixel intensity in the subepithelial region at 20 minutes from three segmentations, and Σpixel $intensity_{cells+se}$ is the combined sum average pixel intensity in the subepithelial and CPE cell regions at 20 minutes from three segmentations.

Statistical Analysis

All imaging experiments were carried out with CP tissues isolated from at least 3 animals. Calculated intensity values were presented as mean ± SD. Statistical significance was determined by using an unpaired Student's t-test or multiple comparisons corrected by the Holm-Sidak method using GraphPad Prism 7. P value less than 0.05 indicated a statistically significant difference.

RESULTS

mRNA Expression of *Abcb1a* (Mdr1a), *Abcb1b* (Mdr1b), and *Abcg2* (Bcrp) in Mouse CP

In mice, there are two isoforms of P-gp, Mdr1a and Mdr1b. We initially determined the mRNA expression the two murine isoforms of P-gp, *Abcb1a* (Mdr1a) and *Abcb1b* (Mdr1b), as well as *Abcg2* (Bcrp) in the lateral ventricle CP of wild-type FVB mice using RT-qPCR (Figure 1). *Abcg2* mRNA is expressed at higher levels than *Abcb1a*, while *Abcb1b* is minimally expressed. The higher expression of *Abcb1a* over *Abcb1b* in choroid plexus is similar to previous findings in whole brain homogenates (24).

Calcein-AM Accumulation in Wild-type and Mdr1a/1b$^{-/-}$ CP

To test the activity of P-gp at the apical CPE cell membrane, real-time uptake of calcein-AM, a P-gp substrate, was performed in CP tissues of wild-type and Mdr1a/1b$^{-/-}$ mice in different inhibitory conditions. Calcein-AM is a non-fluorescent, lipophilic P-gp substrate. After entering the cell by passive diffusion, the compound is cleaved by intracellular esterases to yield the hydrophilic, fluorescent molecule calcein (25,26). When calcein-AM was incubated alone in CP tissues of wild-type mice, the fluorescent calcein was primarily retained intracellularly in the CPE cells (Figure 2 A&E), with a $CPEI_{20min}$ of 18.9 ± 4.1%. When co-incubated with the dual inhibitor elacridar, calcein accumulation increased 468% in the CPE cells compared to the control group (Figure 2 B&F; Figure 3). Intriguingly, coincubation with the Bcrp inhibitor Ko143 also enhanced CPE cell accumulation of calcein, with an increase of 358% compared to treatment with calcein-AM alone (Figure 2 C&G; Figure 3). However, cellular accumulation of calcein did not increase in Mdr1a/1b$^{-/-}$ CP tissues compared to wild-type controls (Figure 2 D&H; Figure 3). No apparent changes

to subepithelial accumulation were observed in wild-type and Mdr1a/1b$^{-/-}$ CP tissues over the time (Figure 2 A&D), whereas in wild-type CP treated with elacridar or Ko143, increases in CPE cell and subepithelial calcein levels were observed (Figure 2 B&C). Taken together, the data suggest that there is a robust Ko143- and elacridar-sensitive transport mechanism at the CSF-facing apical membrane that mediates active efflux of calcein-AM, limiting its entry into the CPE cells. As no change of calcein signal was observed in CP tissues from Mdr1a/1b$^{-/-}$ mice, we tested if Bcrp, which is also expressed apically at the BCSFB and sensitive to these inhibitors (27), may contribute to calcein-AM efflux at the apical membrane of the CPE cells.

CP Transport of BODIPY FL-Prazosin is Sensitive to Ko143

To test the functional activity of Bcrp on the apical membrane, we incubated freshly isolated CP tissues with an established Bcrp substrate, BODIPY FL-Prazosin, in the presence and absence of the Bcrp inhibitor Ko143. When incubated alone in CP tissues, BODIPY FL-Prazosin accumulated primarily in the CPE cells with minimal accumulation in the subepithelial space (Figure 4), with a $CPEI_{20min}$ of 20.5±3.6%. Coincubation with Ko143 increased the CPE cell accumulation of BODIPY FL-Prazosin by 165% (Figure 4), suggesting that Ko143 inhibits apical transport of BODIPY FL-Prazosin in CPE cells and Bcrp could be functionally active at the apical membrane of the BCSFB.

Transport of BODIPY FL-Prazosin in Wild-type and Bcrp$^{-/-}$ CP tissues

As BODIPY FL-Prazosin has also been reported as a P-gp substrate (28), we performed transport studies in CP tissues isolated from wild-type and Bcrp$^{-/-}$ mice. BODIPY FL-Prazosin was incubated in CP tissues of wild-type and Bcrp$^{-/-}$ mice in the presence and absence of elacridar, a dual inhibitor of Bcrp and P-gp (29) (Figure 5). With the dual inhibitor elacridar, we observed a 220% increase in CPE cell accumulation of BODIPY FL-Prazosin in wild-type tissues (Figure 5). In the Bcrp$^{-/-}$ group with no elacridar, a 43% increase was observed in CPE cell accumulation compared to the wild-type CP (Figure 5). BODIPY FL-Prazosin accumulation was further increased in CP tissues of Bcrp$^{-/-}$ mice co-incubated with elacridar, with a 116% increase in CPE cell accumulation compared to wild-type tissues without an inhibitor (Figure 5). This data suggests, ancillary to Bcrp, P-gp may also contribute to apical efflux of BODIPY FL-prazosin at the murine BCSFB. To examine if Bcrp$^{-/-}$ mice exhibited any compensatory changes in P-gp expression in the CP, we additionally quantified the mRNA expression of the murine P-gp isoforms, the *Abcb1a* and *Abcb1b* genes, in CP of wild-type and Bcrp$^{-/-}$ mice. No significant change in mRNA expression of either isoform of P-gp was observed (Figure 6).

DISCUSSION

Earlier research has suggested that Bcrp and P-gp are expressed apically or subapically at the BCSFB (6,7). This CSF-facing localization implies an inward transport function to the brain, which is opposite to their role of restricting brain entry of xenobiotics at the luminal membrane of the BBB. Functional studies on Bcrp and P-gp at the BCSFB are limited and have only been conducted using cultured or immortalized CPE cells that may not preserve the physiology and transporter expression at the BCSFB (17). In this

study, we investigate functional activity of P-gp and Bcrp at the BCSFB using quantitative fluorescence microscopy in freshly isolated CP tissues from wild-type, Mdr1a/1b$^{-/-}$, and Bcrp$^{-/-}$ mice. Our results demonstrated the functional activity of Bcrp at the BCSFB apical membrane and provided evidence supporting a Bcrp-independent, elacridar-sensitive apical efflux mechanism likely mediated by P-gp.

We first confirmed the mRNA expression of P-gp (Mdr1a) and Bcrp in murine CP tissues (Figure 1). To evaluate P-gp activity at the BCSFB, we incubated intact murine CP tissues with calcein-AM, a non-fluorescent, lipophilic P-gp substrate. After entering the cells by passive diffusion, calcein-AM is cleaved by intracellular esterases to generate hydrophilic fluorescent calcein. We found that in wild-type mice, elacridar and Ko143 both strongly inhibited calcein-AM efflux from the CPE cells, resulting in substantial increases in intracellular calcein accumulation in CPE cells (Figures 2 and 3). However, knockout of P-gp had little impact on intracellular calcein accumulation in CPE cells, suggesting a potential involvement of Bcrp or other transporters. Although calcein-AM is not a substrate for human BCRP (30,31), to our knowledge calcein-AM has not been specifically tested with the mouse Bcrp homolog. Additional study is needed to confirm if calcein-AM is indeed transported by the murine Bcrp.

Previous studies have established the expression and activity of Mrp1/4 at the basolateral (blood-facing) membrane of the BCSFB (19,32,33). Calcein is also reported to be a substrate of Mrp1 (34); however, Mrp1, as well as Mrp4, are expressed basolaterally, mediating substrate efflux from the CPE cells into the subepithelial space. Our data revealed that there is little calcein accumulation in the subepithelial space in wild-type CP tissues (Figure 2 A), suggesting a negligible transport of calcein by basolateral Mrp1/4 under the normal conditions. This is most likely due to the low calcein concentrations within wild-type CPE cells due to robust apical efflux of calcein-AM, making few calcein molecules available for basolateral efflux by Mrp1/4. Indeed, when calcein concentrations in CPE cells were increased by either elacridar or Ko143, increases in subepithelial calcein signals were observed (Figure 2 B&C). This can be explained by an appreciable Mrp1/4-mediated basolateral efflux at higher intracellular calcein concentrations.

As our data suggested a possible function of Bcrp at the apical membrane, BODIPY FL-Prazosin, a fluorescent BCRP substrate (27), was then utilized to probe Bcrp activity at the apical membrane of the BCSFB. We observed a 43% increase in CPE cell accumulation of BODIPY FL-Prazosin in Bcrp$^{-/-}$ mice compared to wild-type controls (Figure 5), demonstrating that Bcrp is indeed expressed and functionally active at the apical membrane. Compared to genetic deletion of Bcrp, much larger effects were observed with Ko143 and elacridar which respectively increased BODIPY FL-Prazosin CPE accumulation by 165% and 220% (Figures 4&5). As BODIPY FL-Prazosin is also transported by P-gp, and elacridar is also an inhibitor of P-gp (35), it is likely that P-gp also contributes to BODIPY FL-Prazosin efflux at the apical membrane. Ko143 may be also acting as a dual inhibitor similar to elacridar, rather than a Bcrp-specific inhibitor. Although early studies demonstrate that Ko143 is much more potent for human BCRP compared to human P-gp (36), some evidence suggests that Ko143 can inhibit murine Mdr1a at micromolar concentrations (20 μM) (37), and that Ko143 is transported by Mdr1a at the murine BBB (38). Collectively,

our findings suggest that Bcrp and P-gp are likely both functional at the apical membrane of murine BCSFB; and there may exist a compensatory effect between the two transporters where deletion of one transporter could be partially, or even fully, compensated for by the presence of the other transporter. This compensation is likely to occur at a functional level without incurring transcriptional upregulation since we did not observe a change in Mdr1a/1b CP expression in Bcrp$^{-/-}$ mice (Figure 6).

At the BBB, P-gp and Bcrp are known to 'cooperate' to limit the entry of chemotherapeutic and other shared substrates into the brain (4). When only a single transporter is inhibited or knockout, little or no increase in brain penetration was observed for several dual substrates (39–43). For these compounds, large increases in brain concentrations are only observed when both P-gp and Bcrp are inhibited or knocked out. One example is topotecan, an antineoplastic substrate of both Bcrp and P-gp (40). Brain exposure of topotecan was only marginally (< 1.5 fold) increased in Bcrp$^{-/-}$ mice or Mdr1a/1b$^{-/-}$ mice but increased over 12-fold in P-gp and Bcrp double knockout mice (40). In another study, Lee et al. initially conducted *in situ* brain perfusion of mitoxantrone in wild-type, P-gp$^{-/-}$, and Bcrp$^{-/-}$ mice. Brain mitoxantrone uptake was enhanced with elacridar inhibition but showed no change in either P-gp$^{-/-}$ or Bcrp$^{-/-}$ mice (44). It was in a follow up study, the authors observed that brain penetration of mitoxantrone was greatly increased by ~8-fold in mice lacking both P-gp and Bcrp transporters (45). Thus, a similar synergy may exist between P-gp and Bcrp at the BCSFB; and future investigation using mouse models lacking both transporters would provide further insights on potential functional compensation between P-gp and Bcrp at the BCSFB.

Characterization of BCSFB transport has predominantly been performed in preclinical species, as it is difficult to study BCSFB transport directly in humans and there are limited validated *in vitro* tools for human BCSFB. However, transporter isoforms of preclinical species are poorly characterized relative to their human counterparts, and the expression levels of transporters may also differ between species. Notably, quantitative proteomics studies have shown that P-gp protein expression at the BBB is lower in humans than in rodents whereas BCRP protein levels are higher in humans as compared to mice (46). To our knowledge, broad characterization of transporter protein expression at the BCSFB has not been performed in mice. Bcrp and P-gp proteins have, however, been quantified by limited proteomics work in the CPs of rats and humans (47). Expression of human P-gp is 6-7 fold greater than rat P-gp, while expression of human Bcrp is 2-fold lower than rat Bcrp (47). However, CP tissue from only a single human subject was used in this study, which may not be representative for the general population. Further studies characterizing species differences in transporter expression and function are needed to assess the translational utility of preclinical models towards extrapolating and interpreting human transporter functions at the BCSFB.

The apical localization of Bcrp at the BCSFB implies the transporter mediates entry of compounds into the CSF from the blood. While this localization is peculiar with respect to the barrier function of the BCSFB, another function of the blood-CSF interface is to provide nourishment and maintain healthy brain homeostasis (9). For example, the CP actively transports vitamin C from blood into CSF via the sodium-dependent vitamin C

transport system-1 (48). Several endogenous compounds are substrates of BCRP, including dehydroepiandrosterone sulfate, riboflavin, and folic acid (49). Thus, the apical localization of BCRP may imply a role of BCRP in transporting certain nutrients into the CSF. This function may be especially relevant during early development, as the choroid plexuses receive higher relative blood supply during this period (50).

In summary, studies performed in this work suggest the functional presence of the drug efflux transporters Bcrp and P-gp at the BCSFB. CSF fluid remains the only accessible fluid to sample drug concentrations in the human CNS. However, prediction of free brain concentrations from CSF is challenging and depends on a full understanding of the transport processes at the BBB and BCSFB. More research to understand the contribution of these transporters on brain drug disposition can help our understanding of the relationship between CSF and unbound brain concentrations and improve our predictions of CNS efficacy and toxicity in humans.

CONCLUSIONS

In this study we demonstrated functional activity of Bcrp at the murine BCSFB using quantitative fluorescence microscopy and a genetic knockout mouse model of Bcrp. An additional Bcrp-independent, elacridar-sensitive apical efflux mechanism was detected at the BCSFB, which is likely mediated by P-gp. Findings from this study contribute to the understanding of transport mechanisms that regulate CSF drug concentrations, which is relevant for the prediction and interpretation of CNS pharmacokinetics and pharmacodynamics for CNS drug candidates.

ACKNOWLEDGEMENTS

The authors would like to thank Nathaniel Peters at the UW Keck Microscopy Center for his help and insights in confocal microscopy practice.

FUNDING STATEMENT

This work was supported in part by the National Institutes of Health grant R21 AG071827.

DATA AVAILABILITY

The datasets generated during the current study are available from the corresponding author upon reasonable request.

ABBREVIATIONS

BBB	Blood-brain barrier
BCSFB	Blood-CSF barrier
BCRP/Bcrp	Breast cancer resistance protein
CP	Choroid plexus
CPE cells	Choroid plexus epithelial cells

CPEI	Choroid plexus efflux index
CNS	Central nervous system
CSF	Cerebrospinal fluid
P-gp/MDR1	P-glycoprotein

REFERENCES

1. Feigin VL, Vos T, Nichols E, Owolabi MO, Carroll WM, Dichgans M, et al. The global burden of neurological disorders: translating evidence into policy. The Lancet Neurology. 2020 Mar 1;19(3):255–65. [PubMed: 31813850]
2. Gribkoff VK, Kaczmarek LK. The need for new approaches in CNS drug discovery: Why drugs have failed, and what can be done to improve outcomes. Neuropharmacology. 2017;120:11–9. [PubMed: 26979921]
3. Giacomini KM, Huang SM, Tweedie DJ, Benet LZ, Brouwer KLR, Chu X, et al. Membrane transporters in drug development. Nature Reviews Drug Discovery. 2010;9(3):215–36. [PubMed: 20190787]
4. Agarwal S, Hartz AMS, Elmquist WF, Bauer B. Breast cancer resistance protein and P-glycoprotein in brain cancer: two gatekeepers team up. Current pharmaceutical design. 2011;17(26):2793–802. [PubMed: 21827403]
5. Morris ME, Rodriguez-Cruz V, Felmlee MA. SLC and ABC Transporters: Expression, Localization, and Species Differences at the Blood-Brain and the Blood-Cerebrospinal Fluid Barriers. The AAPS Journal. 2017;19(5):1317–31. [PubMed: 28664465]
6. Rao VV, Dahlheimer JL, Bardgett ME, Snyder AZ, Finch RA, Sartorelli AC, et al. Choroid plexus epithelial expression of MDR1 P glycoprotein and multidrug resistance-associated protein contribute to the blood–cerebrospinal-fluid drug-permeability barrier. Proceedings of the National Academy of Sciences. 1999 Mar 30;96(7):3900 LP – 3905.
7. Tachikawa M, Watanabe M, Hori S, Fukaya M, Ohtsuki S, Asashima T, et al. Distinct spatio-temporal expression of ABCA and ABCG transporters in the developing and adult mouse brain. Journal of Neurochemistry. 2005 Oct 1;95(1):294–304. [PubMed: 16181433]
8. Lun MP, Monuki ES, Lehtinen MK. Development and functions of the choroid plexus-cerebrospinal fluid system. Nature reviews Neuroscience. 2015 Aug;16(8):445–57. [PubMed: 26174708]
9. Sun A, Wang J. Choroid Plexus and Drug Removal Mechanisms. The AAPS Journal. 2021;23(3):61. [PubMed: 33942198]
10. Shen H, Smith DE, Keep RF, Xiang J, Brosius FC. Targeted Disruption of the PEPT2 Gene Markedly Reduces Dipeptide Uptake in Choroid Plexus. Journal of Biological Chemistry. 2003 Feb 14;278(7):4786–91. [PubMed: 12473671]
11. Shen H, Smith DE, Keep RF, Brosius FC. Immunolocalization of the Proton-Coupled Oligopeptide Transporter PEPT2 in Developing Rat Brain. Molecular Pharmaceutics. 2004;1(4):248–56. [PubMed: 15981584]
12. Ocheltree SM, Shen H, Hu Y, Keep RF, Smith DE. Role and Relevance of Peptide Transporter 2 (PEPT2) in the Kidney and Choroid Plexus: In Vivo Studies with Glycylsarcosine in Wild-Type and PEPT2 Knockout Mice. Journal of Pharmacology and Experimental Therapeutics. 2005;315(1):240–7. [PubMed: 15987832]
13. Sweet DH, Miller DS, Pritchard JB, Fujiwara Y, Beier DR, Nigam SK. Impaired Organic Anion Transport in Kidney and Choroid Plexus of Organic Anion Transporter 3 (Oat3 (Slc22a8)) Knockout Mice. Journal of Biological Chemistry. 2002;277(30):26934–43. [PubMed: 12011098]
14. Duan H, Wang J. Impaired monoamine and organic cation uptake in choroid plexus in mice with targeted disruption of the plasma membrane monoamine transporter (Slc29a4) gene. Journal of Biological Chemistry. 2013;288(5):3535–44. [PubMed: 23255610]

15. Zhuang Y, Fraga CH, Hubbard KE, Hagedorn N, Panetta JC, Waters CM, et al. Topotecan Central Nervous System Penetration Is Altered by a Tyrosine Kinase Inhibitor. Cancer Research. 2006 Dec 4;66(23):11305–13. [PubMed: 17145877]

16. Baehr C, Reichel V, Fricker G. Choroid plexus epithelial monolayers – a cell culture model from porcine brain. Cerebrospinal Fluid Research. 2006;3(1):13. [PubMed: 17184532]

17. Kläs J, Wolburg H, Terasaki T, Fricker G, Reichel V. Characterization of immortalized choroid plexus epithelial cell lines for studies of transport processes across the blood-cerebrospinal fluid barrier. Cerebrospinal Fluid Research. 2010;7(11). [PubMed: 20507614]

18. Bernd A, Ott M, Ishikawa H, Schroten H, Schwerk C, Fricker G. Characterization of efflux transport proteins of the human choroid plexus papilloma cell line HIBCPP, a functional in vitro model of the blood-cerebrospinal fluid barrier. Pharmaceutical Research. 2015;32(9):2973–82. [PubMed: 25986174]

19. Hu T, Zha W, Sun A, Wang J. Live Tissue Imaging Reveals Distinct Transcellular Pathways for Organic Cations and Anions at the Blood-Cerebrospinal Fluid Barrier. Mol Pharmacol [Internet]. 2022 Jan 1;101(5):334–42. Available from: http://molpharm.aspetjournals.org/content/early/2022/02/22/molpharm.121.000439.abstract [PubMed: 35193935]

20. Sun A, Wang J. Evaluation of Blood-CSF Barrier Transport by Quantitative Real Time Fluorescence Microscopy. Pharmaceutical Research. 2022;39(7):1469–80. [PubMed: 35411508]

21. Schinkel AH, Mayer U, Wagenaar E, Mol CAAM, van Deemter L, Smit JJM, et al. Normal viability and altered pharmacokinetics in mice lacking mdr1-type (drug-transporting) P-glycoproteins. Proceedings of the National Academy of Sciences. 1997 Apr 15;94(8):4028–33.

22. Jonker JW, Buitelaar M, Wagenaar E, van der Valk MA, Scheffer GL, Scheper RJ, et al. The breast cancer resistance protein protects against a major chlorophyll-derived dietary phototoxin and protoporphyria. Proceedings of the National Academy of Sciences. 2002 Nov 26;99(24):15649–54.

23. Schindelin J, Arganda-Carreras I, Frise E, Kaynig V, Longair M, Pietzsch T, et al. Fiji: an open-source platform for biological-image analysis. Nature Methods. 2012;9(7):676–82. [PubMed: 22743772]

24. Cui YJ, Cheng X, Weaver YM, Klaassen CD. Tissue Distribution, Gender-Divergent Expression, Ontogeny, and Chemical Induction of Multidrug Resistance Transporter Genes (Mdr1a, Mdr1b, Mdr2) in Mice. Drug Metabolism and Disposition. 2009 Jan 1;37(1):203 LP – 210. [PubMed: 18854377]

25. Holló Z, Homolya L, Davis CW, Sarkadi B. Calcein accumulation as a fluorometric functional assay of the multidrug transporter. Biochimica et Biophysica Acta (BBA) - Biomembranes. 1994;1191(2):384–8. [PubMed: 7909692]

26. Glavinas H, von Richter O, Vojnits K, Mehn D, Wilhelm I, Nagy T, et al. Calcein assay: a high-throughput method to assess P-gp inhibition. Xenobiotica. 2011 Aug 1;41(8):712–9. [PubMed: 21657832]

27. Mao Q, Unadkat JD. Role of the Breast Cancer Resistance Protein (BCRP/ABCG2) in Drug Transport—an Update. The AAPS Journal. 2015;17(1):65–82. [PubMed: 25236865]

28. Dey S, Ramachandra M, Pastan I, Gottesman MM, Ambudkar SV. Evidence for two nonidentical drug-interaction sites in the human P-glycoprotein. Proceedings of the National Academy of Sciences. 1997 Sep 30;94(20):10594–9.

29. de Bruin M, Miyake K, Litman T, Robey R, Bates SE. Reversal of resistance by GF120918 in cell lines expressing the ABC half-transporter, MXR. Cancer Letters. 1999;146(2):117–26. [PubMed: 10656616]

30. Mao Q Role of the breast cancer resistance protein (ABCG2) in drug transport. The AAPS Journal. 2005;7(1):E118–33. [PubMed: 16146333]

31. Litman T, Brangi M, Hudson E, Fetsch P, Abati A, Ross DD, et al. The multidrug-resistant phenotype associated with overexpression of the new ABC half-transporter, MXR (ABCG2). Journal of Cell Science. 2000 Jun 1;113(11):2011–21. [PubMed: 10806112]

32. Leggas M, Adachi M, Scheffer GL, Sun D, Wielinga P, Du G, et al. Mrp4 Confers Resistance to Topotecan and Protects the Brain from Chemotherapy. Mol Cell Biol [Internet]. 2004

Sep 1;24(17):7612–21. Available from: http://mcb.asm.org/content/24/17/7612.abstract [PubMed: 15314169]

33. Wijnholds J, de Lange ECM, Scheffer GL, van den Berg DJ, Mol CAAM, van der Valk M, et al. Multidrug resistance protein 1 protects the choroid plexus epithelium and contributes to the blood-cerebrospinal fluid barrier. J Clin Invest [Internet]. 2000 Feb 1;105(3):279–85. Available from: 10.1172/JCI8267 [PubMed: 10675353]
34. Olson DP, Taylor BJ, Ivy SP. Detection of MRP functional activity: Calcein AM but not BCECF AM as a multidrug resistance-related protein (MRP1) substrate. Cytometry. 2001 Apr 15;46(2):105–13. [PubMed: 11309820]
35. Hyafil F, Vergely C, Du Vignaud P, Grand-Perret T. In Vitro and in Vivo Reversal of Multidrug Resistance by GF120918, an Acridonecarboxamide Derivative. Cancer Research. 1993 Oct 1;53(19):4595–602. [PubMed: 8402633]
36. Allen JD, van Loevezijn A, Lakhai JM, van der Valk M, van Tellingen O, Reid G, et al. Potent and Specific Inhibition of the Breast Cancer Resistance Protein Multidrug Transporter in Vitro and in Mouse Intestine by a Novel Analogue of Fumitremorgin C1. Molecular Cancer Therapeutics. 2002 Apr 1;1(6):417–25. [PubMed: 12477054]
37. Weidner LD, Zoghbi SS, Lu S, Shukla S, Ambudkar SV, Pike VW, et al. The Inhibitor Ko143 Is Not Specific for ABCG2. Journal of Pharmacology and Experimental Therapeutics. 2015 Sep 1;354(3):384–93. [PubMed: 26148857]
38. Mairinger S, Zoufal V, Wanek T, Traxl A, Filip T, Sauberer M, et al. Influence of breast cancer resistance protein and P-glycoprotein on tissue distribution and excretion of Ko143 assessed with PET imaging in mice. European Journal of Pharmaceutical Sciences. 2018;115:212–22. [PubMed: 29360507]
39. Polli JW, Olson KL, Chism JP, John-Williams L St., Yeager RL, Woodard SM, et al. An Unexpected Synergist Role of P-Glycoprotein and Breast Cancer Resistance Protein on the Central Nervous System Penetration of the Tyrosine Kinase Inhibitor Lapatinib (N-{3-Chloro-4-[(3-fluorobenzyl)oxy]phenyl}-6-[5-({[2-(methylsulfonyl)ethyl]amino}meth. Drug Metabolism and Disposition. 2009 Feb 1;37(2):439 LP – 442. [PubMed: 19056914]
40. de Vries NA, Zhao J, Kroon E, Buckle T, Beijnen JH, van Tellingen O. P-Glycoprotein and Breast Cancer Resistance Protein: Two Dominant Transporters Working Together in Limiting the Brain Penetration of Topotecan. Clinical Cancer Research. 2007 Nov;13(21):6440–9. [PubMed: 17975156]
41. Chen Y, Agarwal S, Shaik NM, Chen C, Yang Z, Elmquist WF. P-glycoprotein and Breast Cancer Resistance Protein Influence Brain Distribution of Dasatinib. Journal of Pharmacology and Experimental Therapeutics. 2009 Sep 1;330(3):956 LP – 963. [PubMed: 19491323]
42. Agarwal S, Sane R, Gallardo JL, Ohlfest JR, Elmquist WF. Distribution of Gefitinib to the Brain Is Limited by P-glycoprotein (ABCB1) and Breast Cancer Resistance Protein (ABCG2)-Mediated Active Efflux. Journal of Pharmacology and Experimental Therapeutics. 2010 Jul 1;334(1):147 LP – 155. [PubMed: 20421331]
43. Lagas JS, van Waterschoot RAB, Sparidans RW, Wagenaar E, Beijnen JH, Schinkel AH. Breast Cancer Resistance Protein and P-glycoprotein Limit Sorafenib Brain Accumulation. Molecular Cancer Therapeutics. 2010 Feb 9;9(2):319–26. [PubMed: 20103600]
44. Lee YJ, Kusuhara H, Jonker JW, Schinkel AH, Sugiyama Y. Investigation of Efflux Transport of Dehydroepiandrosterone Sulfate and Mitoxantrone at the Mouse Blood-Brain Barrier: A Minor Role of Breast Cancer Resistance Protein. Journal of Pharmacology and Experimental Therapeutics. 2005 Jan 1;312(1):44 LP – 52. [PubMed: 15448171]
45. Kodaira H, Kusuhara H, Ushiki J, Fuse E, Sugiyama Y. Kinetic Analysis of the Cooperation of P-Glycoprotein (P-gp/Abcb1) and Breast Cancer Resistance Protein (Bcrp/Abcg2) in Limiting the Brain and Testis Penetration of Erlotinib, Flavopiridol, and Mitoxantrone. Journal of Pharmacology and Experimental Therapeutics. 2010 Jun 1;333(3):788 LP – 796. [PubMed: 20304939]
46. Uchida Y, Ohtsuki S, Katsukura Y, Ikeda C, Suzuki T, Kamiie J, et al. Quantitative targeted absolute proteomics of human blood–brain barrier transporters and receptors. Journal of Neurochemistry. 2011 Apr 1;117(2):333–45. [PubMed: 21291474]

47. Uchida Y, Zhang Z, Tachikawa M, Terasaki T. Quantitative targeted absolute proteomics of rat blood-cerebrospinal fluid barrier transporters: Comparison with a human specimen. Journal of Neurochemistry. 2015;134(6):1104–15. [PubMed: 25951748]

48. Spector R, Robert Snodgrass S, Johanson CE. A balanced view of the cerebrospinal fluid composition and functions: Focus on adult humans. Experimental Neurology. 2015;273:57–68. [PubMed: 26247808]

49. Jani M, Ambrus C, Magnan R, Jakab KT, Beéry E, Zolnerciks JK, et al. Structure and function of BCRP, a broad specificity transporter of xenobiotics and endobiotics. Archives of Toxicology. 2014;88(6):1205–48. [PubMed: 24777822]

50. Ghersi-Egea JF, Vasiljevic A, Blondel S, Strazielle N. Neuroprotective Mechanisms at the Blood-CSF Barrier of the Developing and Adult Brain BT - Role of the Choroid Plexus in Health and Disease. In: Praetorius J, Blazer-Yost B, Damkier H, editors. New York, NY: Springer US; 2020. p. 193–207.

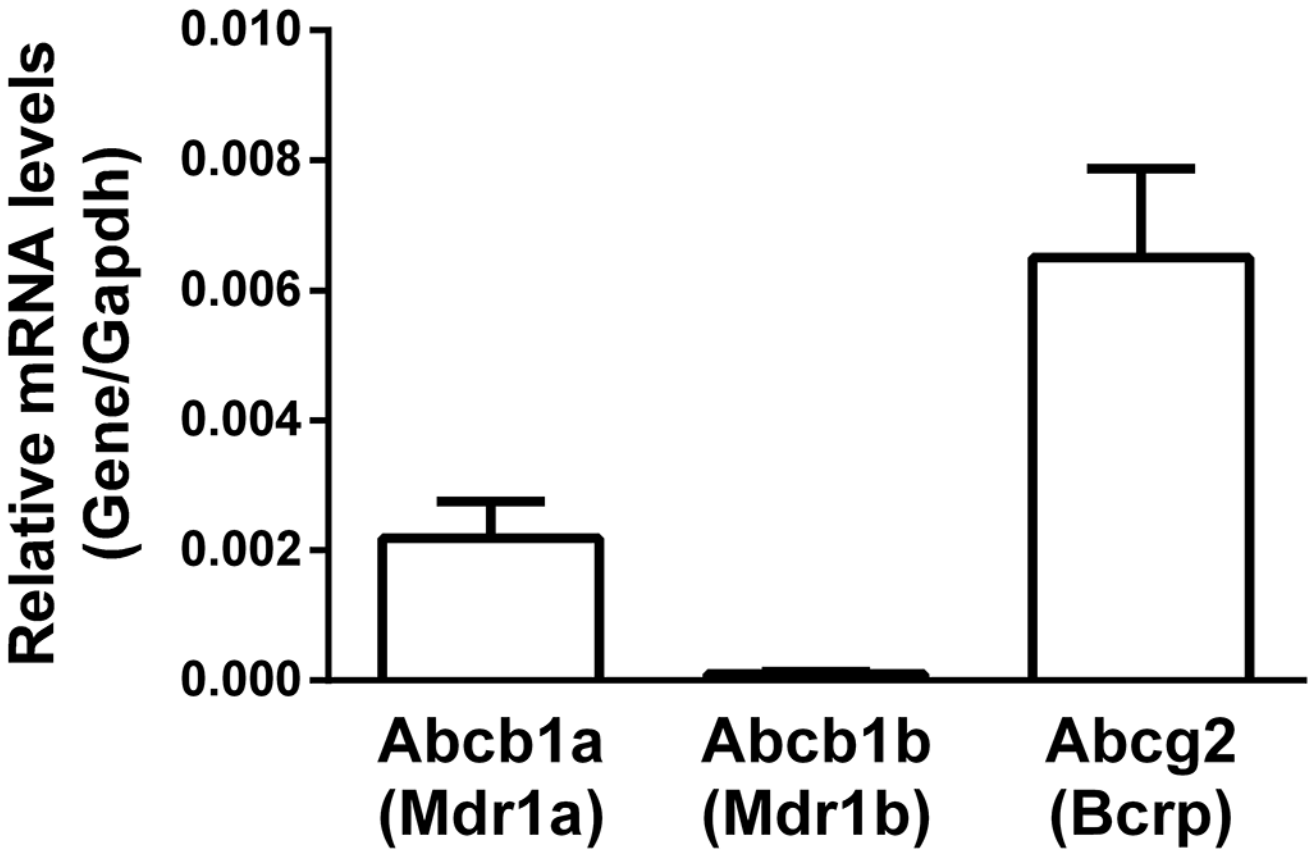

Figure 1.

Relative mRNA expression of *Abcb1a* (Mdr1a), *Abcb1b* (Mdr1b), and *Abcg2* (Bcrp) transporters in FVB mouse lateral ventricle CP tissues (n=9, pooled groups of 3). Expression levels are normalized to the housekeeping gene *Gapdh*. Values are means ± SD across 3 pools of tissues, with each pool containing CP tissues from 3 mice.

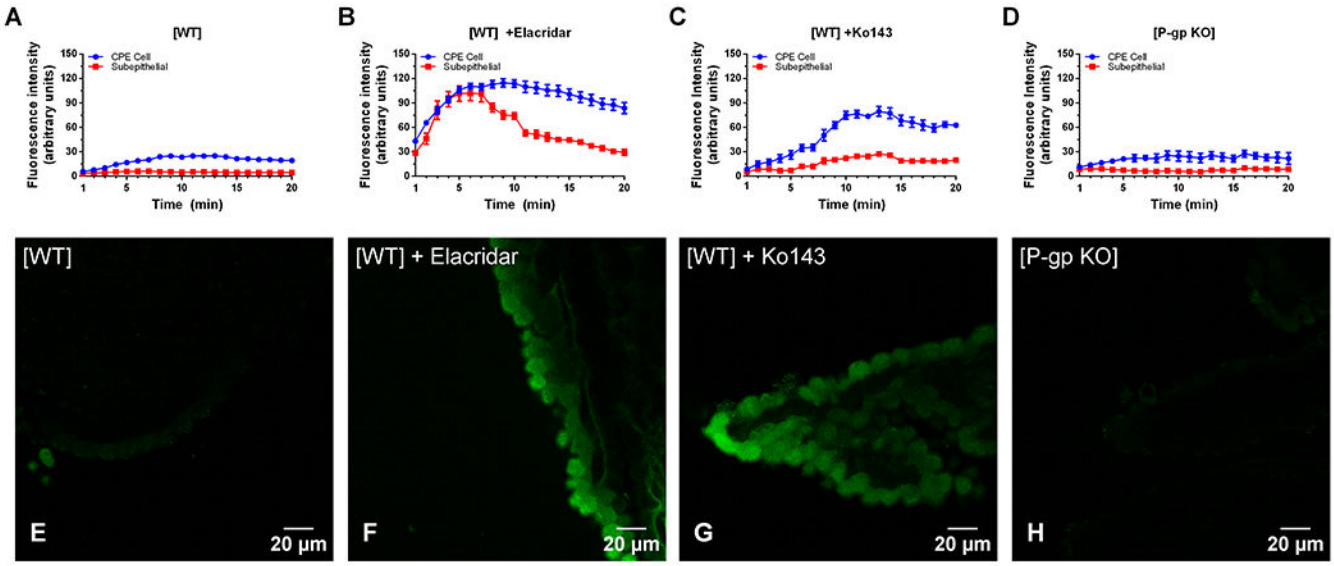

Figure 2.

CP tissues were incubated with 2 µM calcein-AM for 20 minutes in different experimental conditions. Experiments were performed independently in CP tissues from 3 to 9 mice, and results from one representative experiment were shown. Representative time courses of calcein accumulation in CPE cells and subepithelial compartments from individual CP tissues obtained from wild-type mice in (A) the absence of an inhibitor, (B) the presence of 2 µM elacridar, (C) the presence of 1 µM Ko143, and (D) from CP obtained from Mdr1a/1b$^{-/-}$ mice in the absence of an inhibitor. Representative confocal images of calcein accumulation after 20 minutes in CP tissues from wild-type mice in (E) absence of an inhibitor, (F) presence of 2 µM elacridar, (G) presence of 1 µM Ko143, and (H) from CP obtained from Mdr1a/1b$^{-/-}$ mice in the absence of an inhibitor.

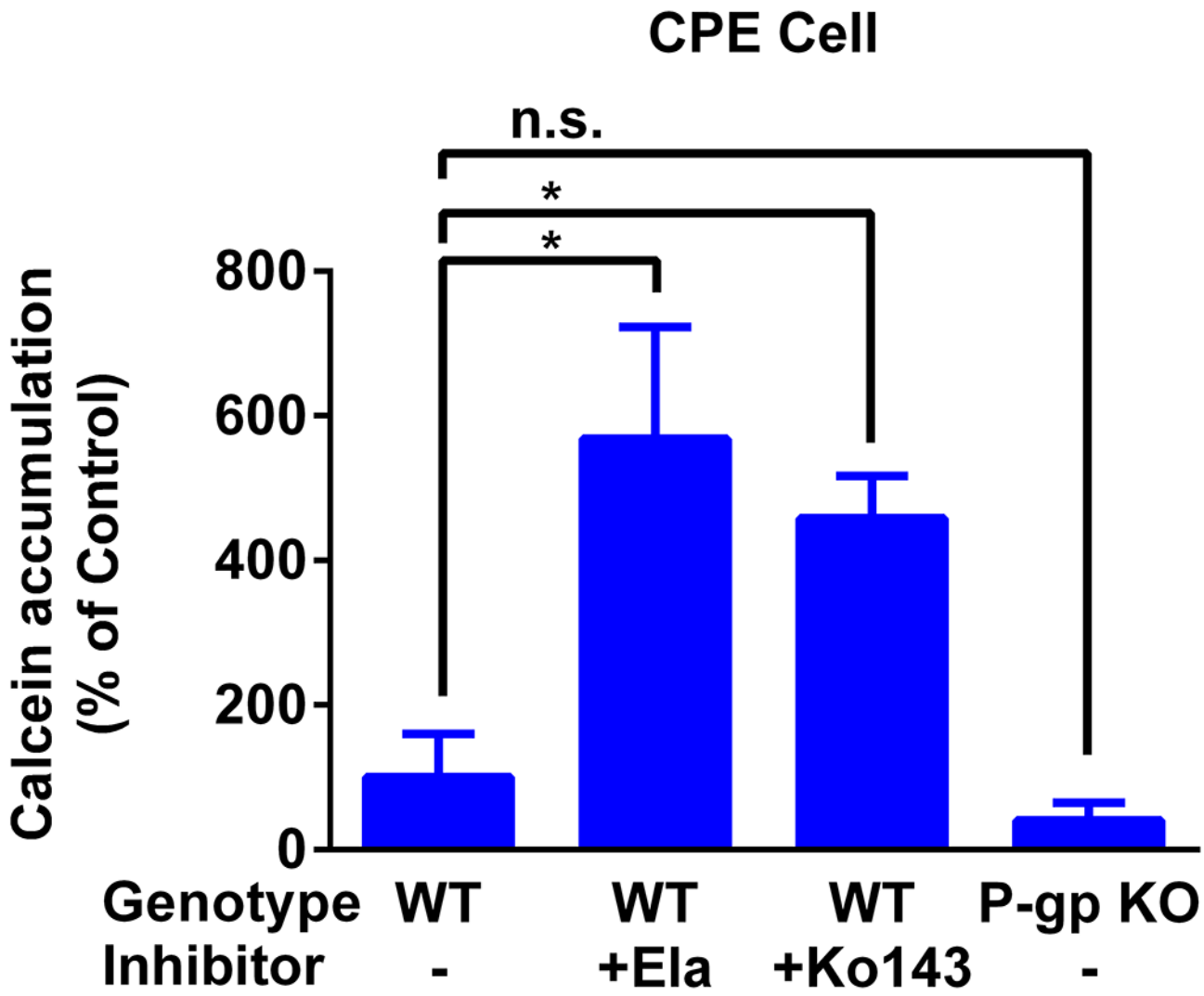

Figure 3.

Quantified changes in CPE cell accumulation under different inhibitory conditions and between CP tissues of wild-type and Mdr1a/1b$^{-/-}$ mice. Data are normalized to calcein CPE cell accumulation with no inhibitor in wild-type tissues. Values are means ± SD across 3-9 mice for all treatment groups.

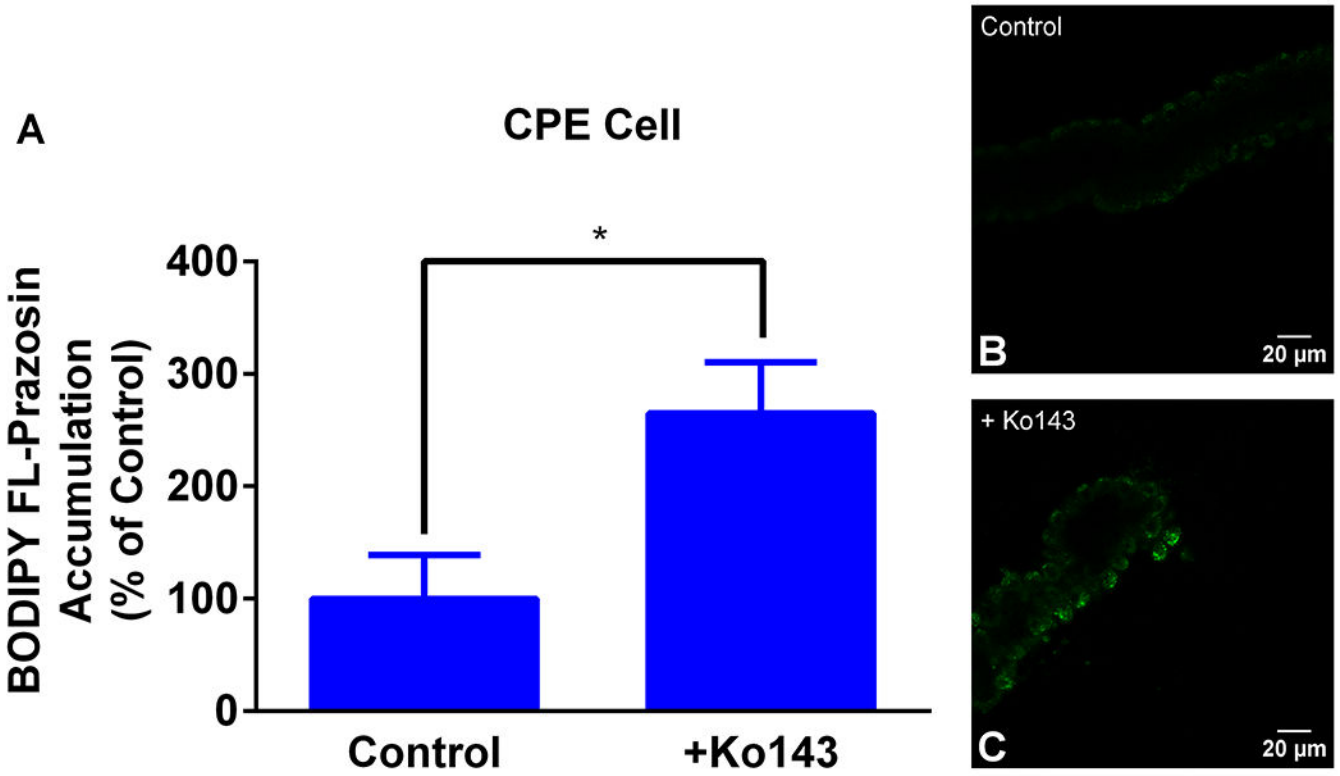

Figure 4.

(A) Change in BODIPY FL-Prazosin accumulation in CPE cells after 20 minutes with and without Ko143. Tissues were incubated with BODIPY FL-Prazosin (2 µM) in the presence or absence of Ko143 (1 µM). Data are normalized to BODIPY FL-Prazosin accumulation in tissues with no inhibitor added. Values are means ± SD across 3 mice for all treatment groups. Representative images of CP tissues taken at 20 minutes in the (B) absence or (C) presence of Ko143.

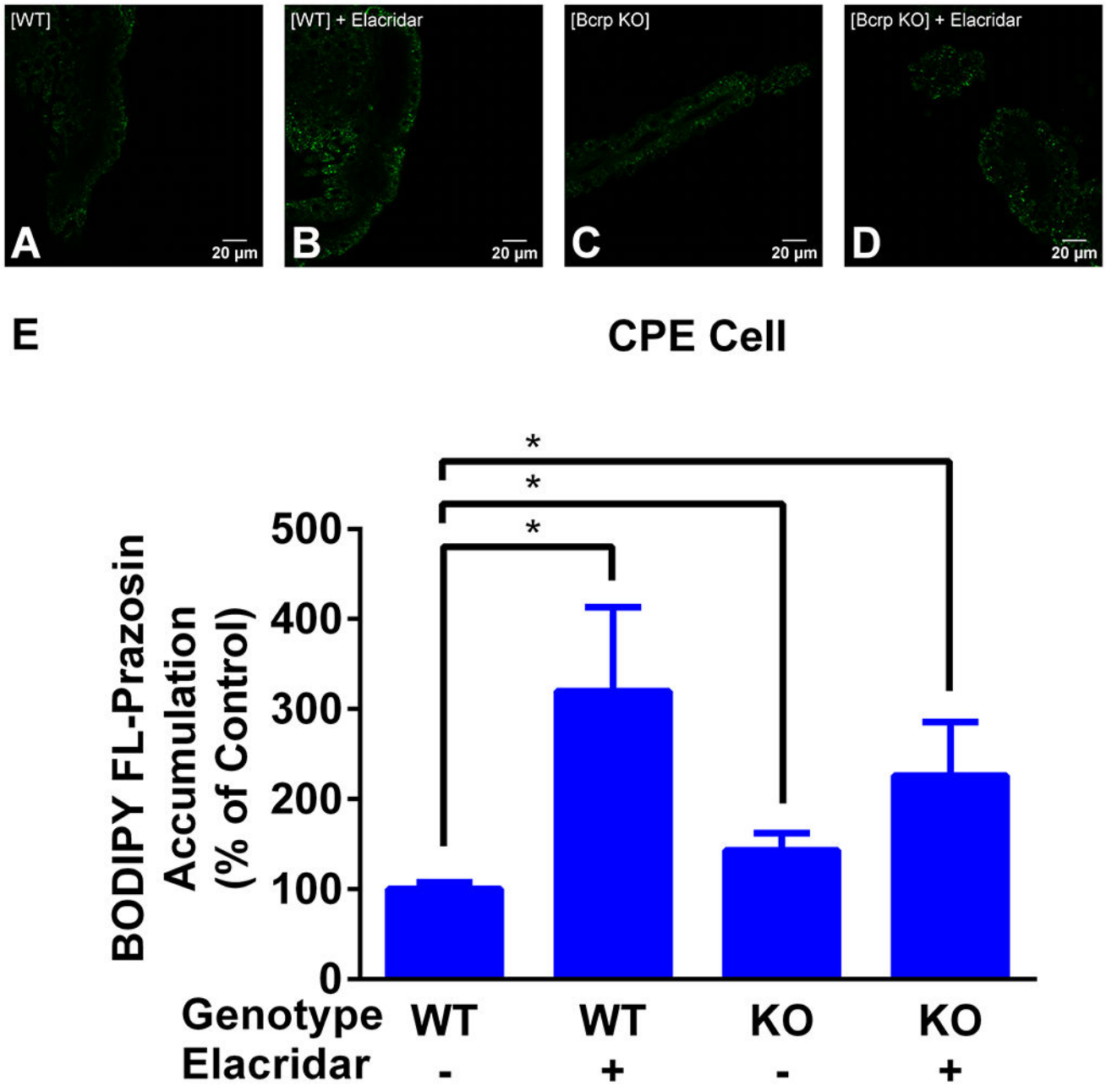

Figure 5.

(A) Representative confocal images of BODIPY FL-Prazosin (2 µM) accumulation in CPE cells of age-matched wild-type mice in the (A) absence and (B) presence of elacridar (2 µM) and of Bcrp$^{-/-}$ mice in (C) absence and (D) presence of elacridar (2 µM). (E) Changes in CPE cell accumulation between treatment groups. Data are normalized to BODIPY FL-Prazosin CPE cell accumulation with no inhibitor in wild-type tissues. BODIPY FL-Prazosin accumulation in other treatment groups were compared to that in wild-type tissues with no elacridar (*P<0.05). Accumulation of BODIPY FL-Prazosin was also compared

between knockout tissues in the absence or presence of elacridar (†P=0.073). Values are means ± SD across 3-4 mice for all treatment groups.

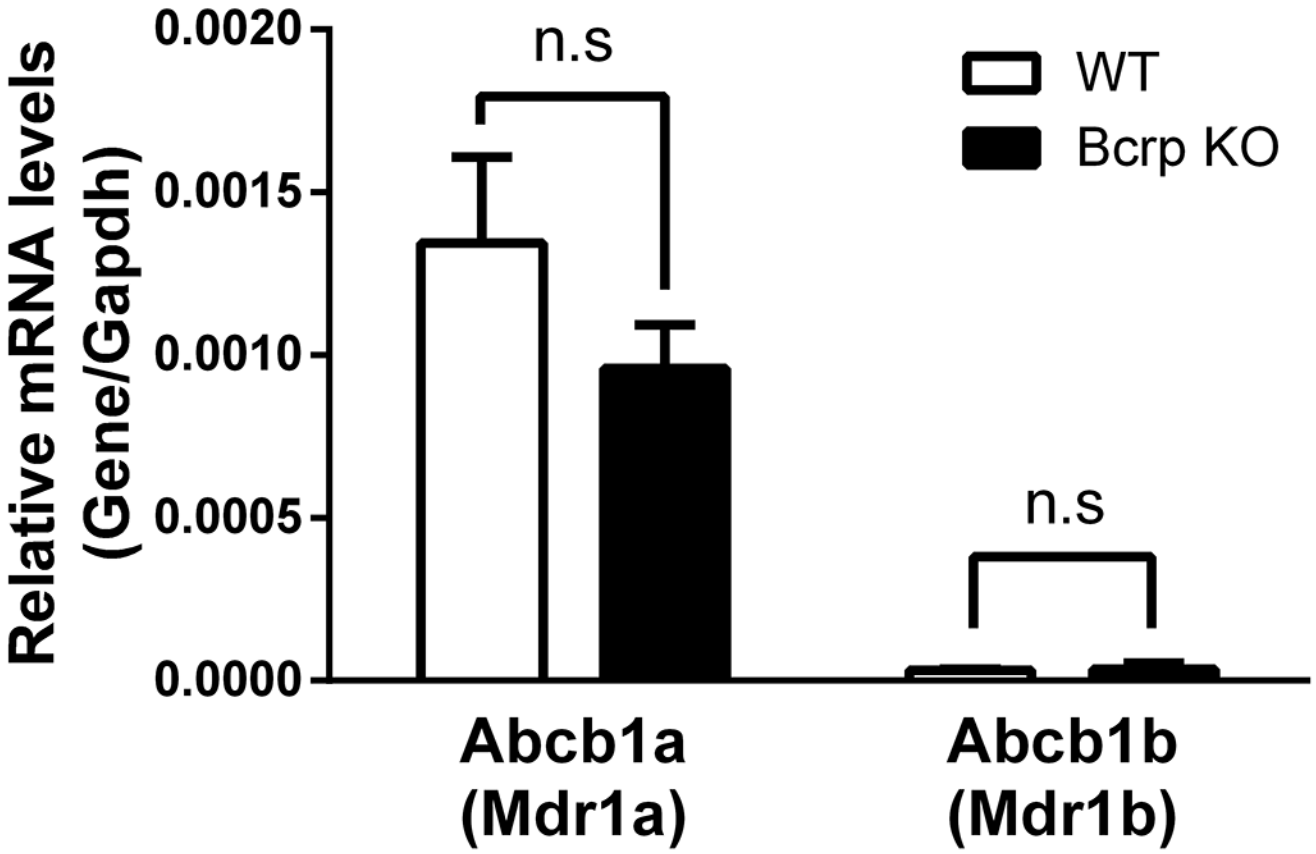

Figure 6.

Relative mRNA expression of the P-gp isoforms *Abcb1a* (Mdr1a) and *Abcb1b* (Mdr1b) in mouse 4th ventricle CP tissues of wild-type and Bcrp$^{-/-}$. Expression levels are normalized to the housekeeping gene *Gapdh*. Values are means ± SD across CP tissues from 3 mice.